Orogen-perpendicular magnetic segmentation of the western Yukon and eastern Alaska cordilleran hinterland: Implications for structural control of mineralization

Matías G. Sánchez[1], Murray M. Allan, Craig J.R. Hart, Jim K. Mortensen
Mineral Deposit Research Unit (MDRU), University of British Columbia, Vancouver, BC

Sanchez, M.G., Allan, M.M., Hart, C.J.R., and Mortensen, J.K., 2013. Orogen-perpendicular magnetic segmentation of the western Yukon and eastern Alaska cordilleran hinterland: Implications for structural control of mineralization. *In:* Yukon Exploration and Geology 2012, K.E. MacFarlane, M.G. Nordling, and P.J. Sack (eds.), Yukon Geological Survey, p. 133-146.

ABSTRACT

This contribution focuses on the analysis, characterization, and mineralization control of northeast-southwest oriented, magnetic heterogeneities of the allochthonous to parautochthonous Intermontane terranes of the North American Cordillera of western Yukon and eastern Alaska. Our interpretation of publically available magnetic datasets proposes sixteen zones of linear discontinuities oriented semi-perpendicular to the northwest-southeast Cordilleran deformation front and mid-Cretaceous Dawson Range magmatic arc. These magnetite-destructive corridors are interpreted as steeply dipping, brittle fault zones and fracture arrays of extensional, oblique-extensional, and strike-slip kinematics responsible for localized structural damage. Their spatial correlation with known mid to Late Cretaceous magmatic-hydrothermal mineralization suggests a first-order structural control in eastern Alaska, while a secondary role is interpreted for Yukon's Dawson Range.

[1]*msanchez@eos.ubc.ca*

INTRODUCTION

Across the western North American Laurentian margin, and specifically along the Canadian Cordillera, orogen-perpendicular, northeast-trending basement and upper crustal fault systems have been interpreted from regional aeromagnetic surveys (Logan *et al.*, 2010; Crawford *et al.*, 2010). We investigate this class of structure in the northern Yukon-Tanana terrane of west-central Yukon and east-central Alaska, using a seamless reduced-to-pole (RTP) magnetic grid generated by Fathom Geophysics LLC (Fig. 1; Buckingham and Core, 2012). The magnetic dataset is a compilation of publically available regional datasets from the U. S. Geological Survey (USGS), Alaska Division of Geological and Geophysical Surveys (DGGS), and Natural Resources Canada (NRCan).

Airborne magnetic surveys constitute one of the most widely used geophysical techniques for mineral exploration and geological interpretation (Gunn and Denith, 1997; Nabighian *et al.*, 2005; Purucker and Clark, 2011). Particular examples of its applications to western North American geology and structure include: (1) the mapping of strong magnetic anomalies caused by buried basement and cratonic structures (Crawford *et al.*, 2010); (2) analysis of weak signals assigned to Laurentian margin sedimentary basins (Lund, 2008); (3) mapping of high amplitude anomalies caused by buried Early Proterozoic magmatic arcs (Pilkington and Saltus, 2009); and (4) mineral exploration applications including the identification of structural controls on Mesoproterozoic massive sulphide and intrusion and fault-related Ag-Pb-Zn and Cu-Ag veins, as well as controls on Mesozoic lode gold and stratabound Cu-Ag deposits (McMechan, 2012). These and other applied magnetics studies have substantially contributed to the understanding of western North America's crustal structure and tectonic evolution (*e.g.*, Pilkington, *et al.*, 2006; Saltus, 2007).

Linear magnetic discontinuities have long been used as a guide to regional structural controls on magmatic-related mineralization within metallogenic provinces of diverse geological settings (*e.g.*, Domzalski, 1966; Henley and Adams, 1992; Sandirin *et al.*, 2007). In this study, we interpret linear magnetic discontinuities, mainly of magnetite-destructive character, corresponding to steeply dipping structures relevant to the structural control of magmatically-related mineralization. Structures of steeply dipping geometries, commonly of extensional or strike-slip kinematics, have frequently been correlated to the distribution of porphyry, mesothermal, and epithermal style mineralization (Hedenquist, 1996; Micklethwaite *et al.*, 2010; Sillitoe, 1997). World-class epithermal deposits controlled by normal faulting include the Comstock Lode in Nevada (Vikre, 1989), Hishikari in Japan (Izawa *et al.*, 1990) and the Kelian deposit in Indonesia (Van Leeuwen *et al.*, 1990). Epithermal mineralization associated with strike-slip systems include the Virginia City and Goldfield mining districts in Nevada (Berger, 2007), Mesquite mining district in southeast California (Willis and Tosdal, 1992), and the Baguio deposit in the Philippines (Cooke *et al.*, 1996; Sillitoe, 1997). Cases of steeply dipping faults controlling mineralization in mesothermal conditions include the strike-slip systems at St Ives goldfield and the Yilgarn craton of Western Australia (Cox, 1999; Cox and Running, 2004). At deeper crustal levels and elevated pressure-temperature conditions, regional scale, steeply dipping fault systems, such as the West Fissure in northern Chile, are broadly accepted to exert a first order structural control on some of the planet's largest porphyry copper deposits (Sillitoe, 1997).

We emphasize the spatial correlation between such linear magnetic discontinuities and the distribution of known Cretaceous magmatic related mineralization in western Yukon and eastern Alaska. The structural interpretation of regional geophysical datasets is part of a larger collaborative venture between the mining exploration industry and the Mineral Deposit Research Unit (MDRU) to improve constraints on metallogeny and generate knowledge relevant to mineral exploration in the region.

TECTONIC AND GEOLOGICAL SETTING

The interpreted magnetic dataset covers an area in the Intermontane terranes of the North American Cordillera of western Yukon and eastern Alaska between two Early Cenozoic, continental-scale dextral strike-slip faults, the Tintina and Denali faults (Fig. 1; Gabrielse *et al.*, 2006). This tectonic zone consists of a series of accreted parautochthonous to allochthonous terranes, including Slide Mountain, Quesnellia, Stikinia, and Yukon-Tanana terranes (Fig. 1; Mortensen, 1992; Colpron *et al.* 2007). The latter represents a mid to Late Paleozoic continental arc that was separated from the western margin of Laurentia by the coeval Slide Mountain back-arc basin during Late Devonian and Early to Middle Triassic time (Nelson *et al.*, 2006). The geometric array of the Intermontane terranes exhibit an overall semi-concentric distribution of mainly magmatic arc rocks, sedimentary

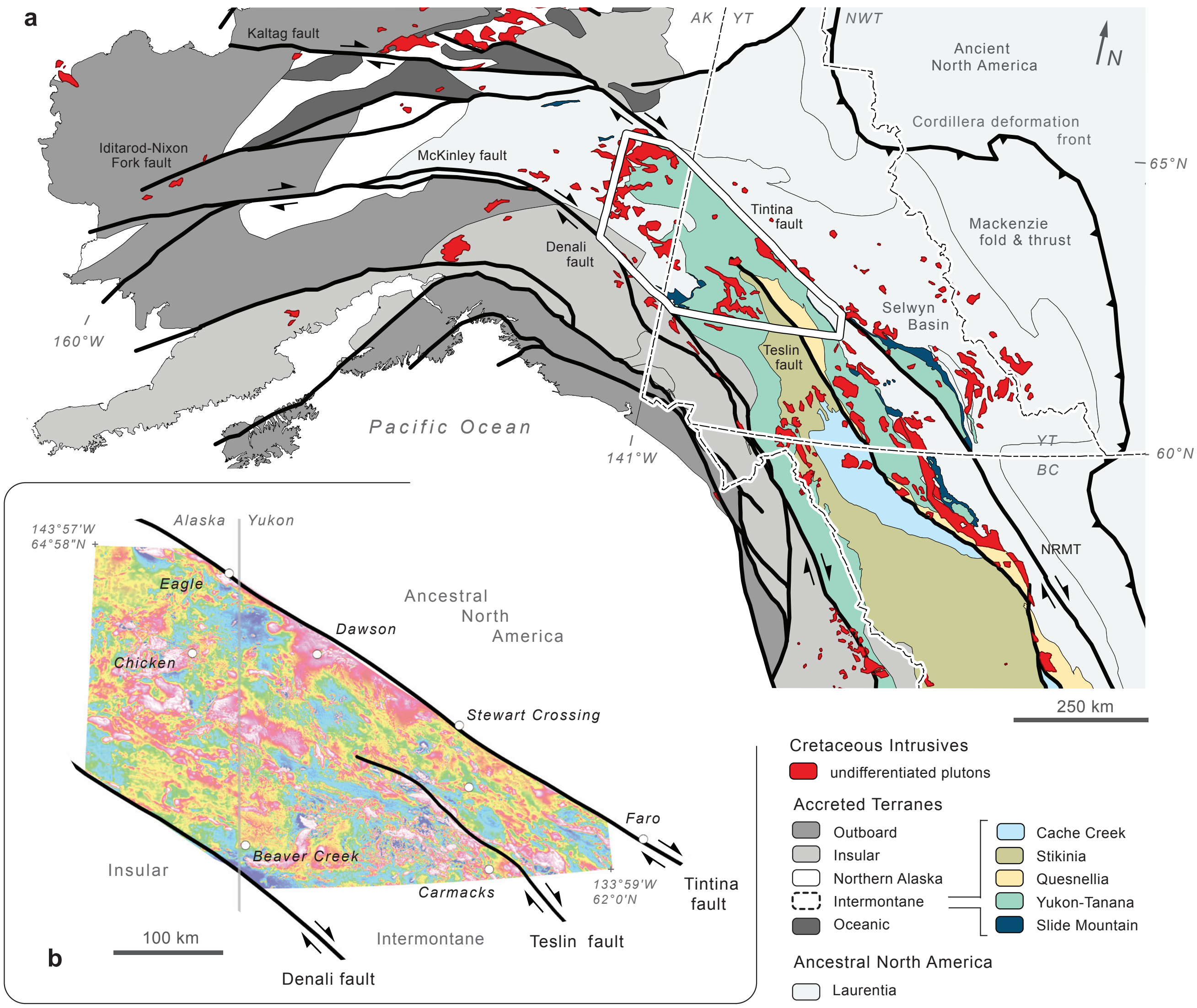

Figure 1. *(a) Tectonic map of the northern North American Cordillera, showing major tectonic boundaries (after Colpron, 2011) and Cretaceous post-accretionary intrusions (Garrity and Soller, 2009). (b) Location of the reduced-to-pole (RTP) magnetic grid.*

successions, and oceanic rocks bordering western Laurentia between mid-Paleozoic to Early Mesozoic times (Colpron *et al.*, 2007). In south-central Yukon, the exotic, Tethyan affinity oceanic rocks of the Cache Creek terrane comprise the core of the Intermontane terranes (Fig. 1; Cordey *et al.*, 1987). Its particular tectonic position has been proposed as the result of oroclinal entrapment by Quesnellia and Stikinia in Early Jurassic time (Mihalynuk *et al.*, 1992, 1994).

Early to Middle Jurassic accretion of the Intermontane terranes to the Laurentian margin, and related northwest-directed, margin-parallel shortening and fast cooling of upper plate rocks, locally switched to southeast-directed crustal extension by Early to mid-Cretaceous time (Dusel-Bacon *et al.,* 2002). In late Early Cretaceous time, extensional footwall exhumation took place in eastern Alaska (Dusel-Bacon *et al.,* 2002), whereas deformation in southern Yukon and northern British Columbia was dominated by dextral strike-slip displacement along the Northern Rocky Mountain Trench (NRMT) and Teslin fault (Fig. 1; Gabrielse *et al.*, 2006). During Early Cenozoic time (mainly Eocene) the Tintina fault propagated as a northern fault segment of the NRMT through Yukon and eastern Alaska (Gabrielse, 1985; Gabrielse *et al.*, 2006). Tectonic restoration of the ~490 km dextral displacement along the Tintina fault to its pre-Cenozoic position, locates the study area within the hinterland zone of the Jurassic-Cretaceous Mackenzie fold and thrust belt to the northeast (Fig.1; Saltus, 2007).

Post-accretionary plutonic suites, caused by Cretaceous to Paleogene convergence, mainly intrude the Intermontane terranes and to a lesser extent the Laurentian margin and Insular terranes (Fig.1; Gabrielse *et al.*, 2006; Mair *et al.*, 2006). Early and mid-Cretaceous magmatism was widespread throughout Alaska and Yukon, with highly oxidized plutonic suites running in a northwest-southeast orientation and orogen-parallel (Fig. 1; Hart *et al.*, 2004; Mair *et al.*, 2006). In the study area, I-type plutons of the *ca.* 110-103 Ma Whitehorse plutonic suite are developed along the Dawson Range, while reduced coeval plutons occur across the back-arc (Fig. 2; Mortensen *et al.*, 2000; Baker and Lang, 2001).

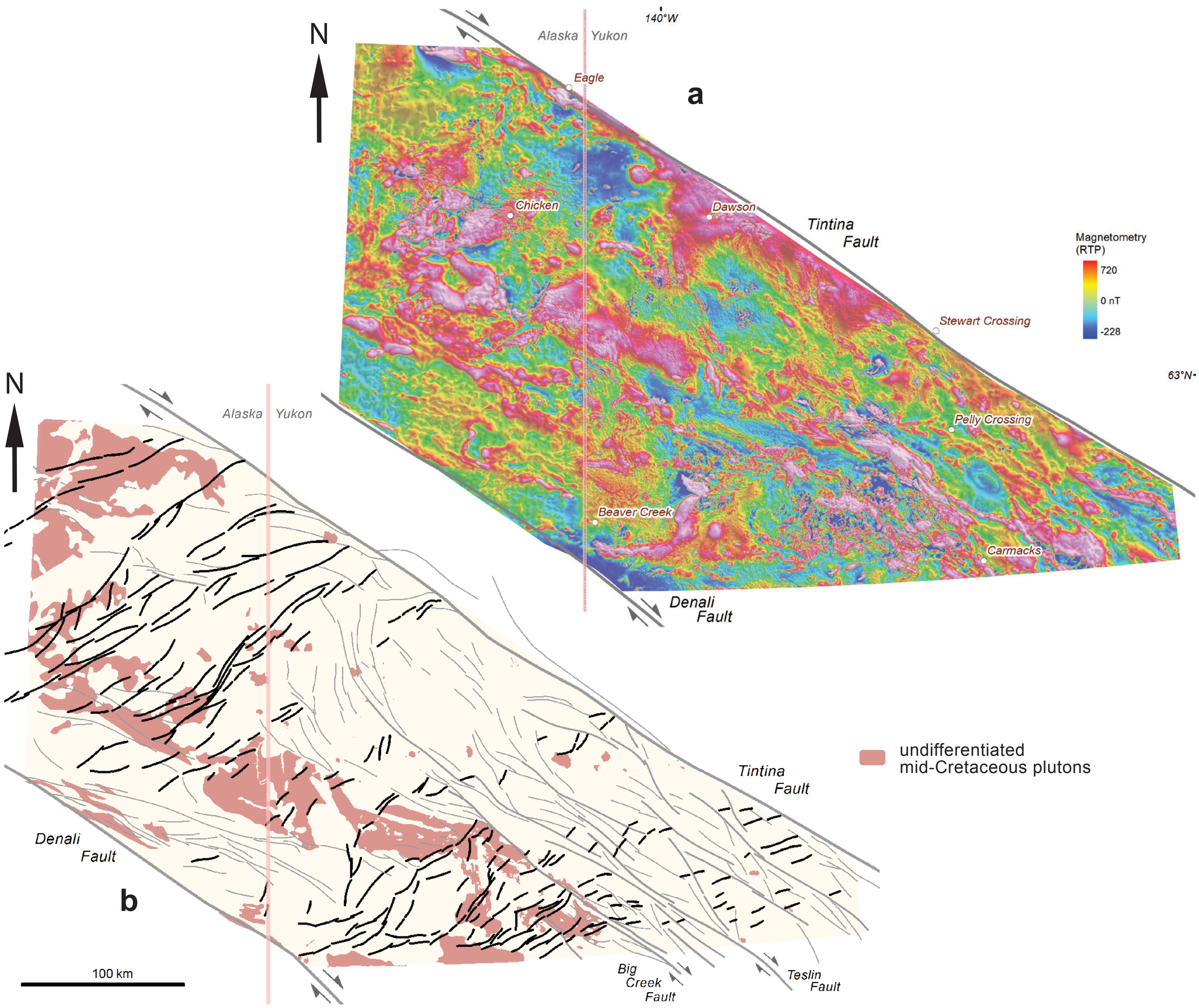

Figure 2. *(a) The levelled reduced-to-pole (RTP) magnetic grid generated by Fathom Geophysics LLC (Buckingham and Core, 2012). (b) Simplified map showing major magnetic discontinuities and magnetite-destructive lineaments of the magnetic dataset. Mid-Cretaceous plutonic rocks from the Whitehorse plutonic suite are shown in grey (modified from Gordey et al., 2005; Ryan et al., 2010; Beikman et al., 1980; and Gordey and Makepeace, 1999).*

METHODOLOGY

The magnetic dataset used in this study spans the northern Yukon-Tanana terrane and consists of a single, seamless reduced-to-pole (RTP) grid, with a 100 m grid cell for Alaska and Yukon (Buckingham and Core, 2012; Figs. 1 and 2). Source data includes regional datasets from the U.S. Geological Survey (USGS), Alaska Division of Geological and Geophysical Surveys (DGGS), and the recent NRCan Yukon Plateau compilation (Hayward *et al.*, 2011). Interpretation was carried out at a maximum scale of 1:300 000 and within a geographic information system platform (ArcGIS 10).

The current study focuses exclusively on linear magnetic discontinuities oriented at high angles to the regional northwest-southeast and orogen-parallel magnetic fabric (Fig. 2). Northwest-oriented magnetic signals correlate to the geometries of major geological contacts, the orientation of the Cretaceous magmatic arc, and to the presence of orogen-parallel fault systems. In the study area, orogen-perpendicular, linear, magnetic discontinuities are observed as magnetite-destruction trends of high-frequency and low-amplitude signals, which commonly border areas of distinct magnetic character (Fig. 3). Although our interpretation follows a similar methodology to ones previously reported (*e.g.*, Grant, 1985), we further emphasize a petrophysical approach (Clark, 1999; Clark *et al.*, 2004; Purucker and Clark, 2011). Our methodology considers common magnetic susceptibility ranges for rock types published in regional geological maps, as well as our own field measurements of magnetic susceptibility. Furthermore, end-member intensities of positive and

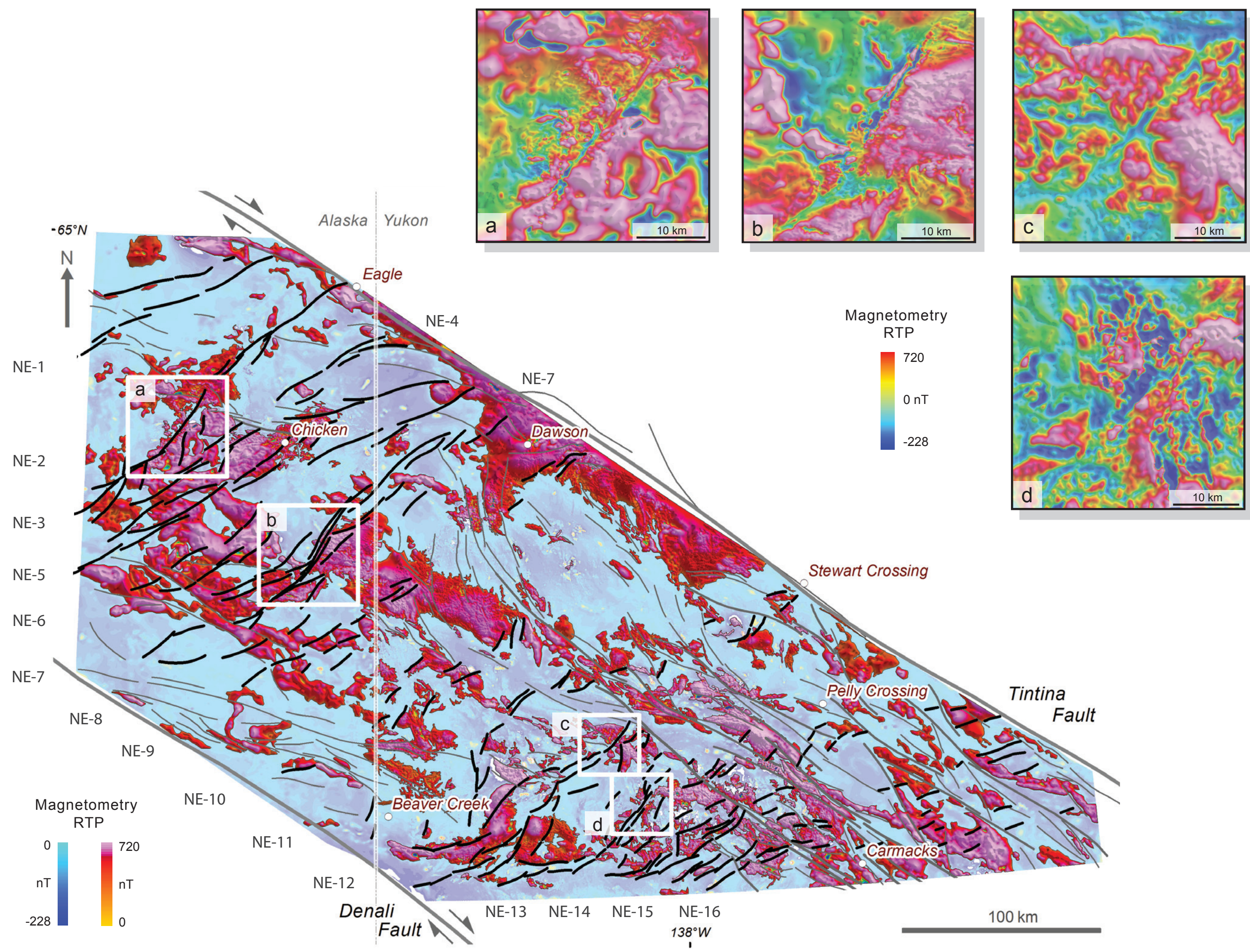

__Figure 3.__ Map-view examples of northeast-trending magnetic discontinuities of the reduced-to-pole grid. Bottom-left corner: Magnetic breaks and offsets in relation to extracted positive magnetic anomalies. Upper-right corner: Key examples of northeast-trending magnetite-destructive lineaments: (a) Ketchumstuk; (b) Sixtymile-Pika; (c) Dip Creek; and (d) Selwyn River.

negative magnetic anomalies, as well as a series of range domains, were extracted from the RTP grid and compared to distinctive rock susceptibilities (*e.g.*, ultramafic rocks, magnetite-series plutonic suites) (Fig. 3).

The main objective in our structural-magnetometric interpretation focuses on the generation of a magnetic discontinuity map. This process consists of four main stages, beginning with tracing major linear features and discontinuities in the RTP magnetic grid (*i.e.*, magnetite-destructive lineaments and long axes of major magnetic anomalies). In the second stage, lineaments are compared against major structural geomorphology features from digital elevation models (regional 1 km resolution GEBCO 08 DEM and 30 m resolution Aster GDEM). In the third stage, possible structural offsets of geological contacts are evaluated from regional geological maps (Gordey and Ryan, 2005; Ryan *et al.*, 2010; Beikman *et al.*, 1980; Gordey and Makepeace, 1999). During the magnetic discontinuity map construction, a binary value is assigned to individual lineaments, according to whether they are also expressed in remote sensing datasets and geological maps. This quantified approach to multi-dataset interpretation results in a probability scale from which the most probable structures can be determined. Most plausible structures are represented by large scale magnetite-destructive lineaments, showing visible offsets of magnetic anomalies and geological contacts. These are commonly accompanied by a topographic trench and rarely offset drainages. In the final stage, lineaments have been grouped into sixteen zones of magnetic discontinuities according to their spatial distribution and density. These have been named consecutively, from north to south, as NE-1 to NE-16 (Fig. 3).

REGIONAL NE-SW MAGNETIC DISCONTINUITIES

Northeast-trending corridors of linear magnetite-destructive discontinuities truncate and offset some of the most prominent orogen and arc-parallel northwest-southeast oriented magnetic trends (Fig. 2). These high frequency and low intensity magnetic discontinuities are interpreted as the consequence of steeply-dipping fault systems oriented near perpendicular to the main regional magnetic signals (Fig. 3). Individual northeast oriented structural systems are composed of a series of linear segments of ~3 to 50 km in length that link and relay along strike. While these appear highly continuous and linear across the Alaskan part of the magnetometric grid, arcuate and highly segmented arrays commonly occur in the Yukon segment (Figs. 3 and 4). These regional geometric variations may result from shallower dips on fault surfaces in Yukon compared with steeper dips in Alaska. Major structural offsets and block segmentation are made evident when high intensity anomalies are extracted from the RTP dataset (Fig. 3). When the spatial distribution of lineaments and geological map units are compared, it is deduced that a series of major geological map patterns are constrained by northeast-southwest magnetic discontinuity corridors. An outstanding example is given by the along-strike block segmentation of the areal exposure of mid-Cretaceous igneous rocks of the Whitehorse plutonic suite (Fig. 2 and 5).

ALASKAN AREA

Across the Alaskan portion of the RTP magnetic grid, approximately eight major fault-fracture systems show highly continuous and linear patterns with major discontinuity zones reaching up to ~180 km in length (Figs. 2 and 4). Regional northeast-southwest oriented linear magnetic discontinuities are evident across the entire width of the Intermontane terrane block, *i.e.*, extending from the Denali to Tintina faults. Discrete, linear, magnetite-destructive discontinuities of up to ~60 km in length are responsible for the apparent truncation of orogen and arc-parallel shallow magnetic sources, as well as northwest-southeast elongated, high amplitude anomalies.

The most prominent magnetic truncations and offsets of high amplitude anomalies are observed in the Alaskan part of the study area. For example, a major geological and magnetic truncation is observed along the western edge of the Fortymile District, in Alaska, where the Ketchumstuk fault system runs for ~110 km in a northeast-southwest orientation (NE-3 in Figure 4a). This highly continuous structural system is composed of a linear central fault zone and associated oblique north-south oriented faults developed along a band of mid-Cretaceous intrusive rocks of the Whitehorse plutonic suite. Farther along strike to the north-east, this linear magnetic discontinuity defines the fault-bound margins of Late Triassic to Early Jurassic intrusions (Fig. 5). At least seven other regional scale discontinuities of similar orientation have been interpreted across the Alaskan portion of the RTP grid (Fig. 3). Additional examples of plan-view offsets of high amplitude anomalies, associated with mid-Cretaceous, oxidized plutonic rocks, are observed across NE-2 and NE-7 (Figs. 3 and 4).

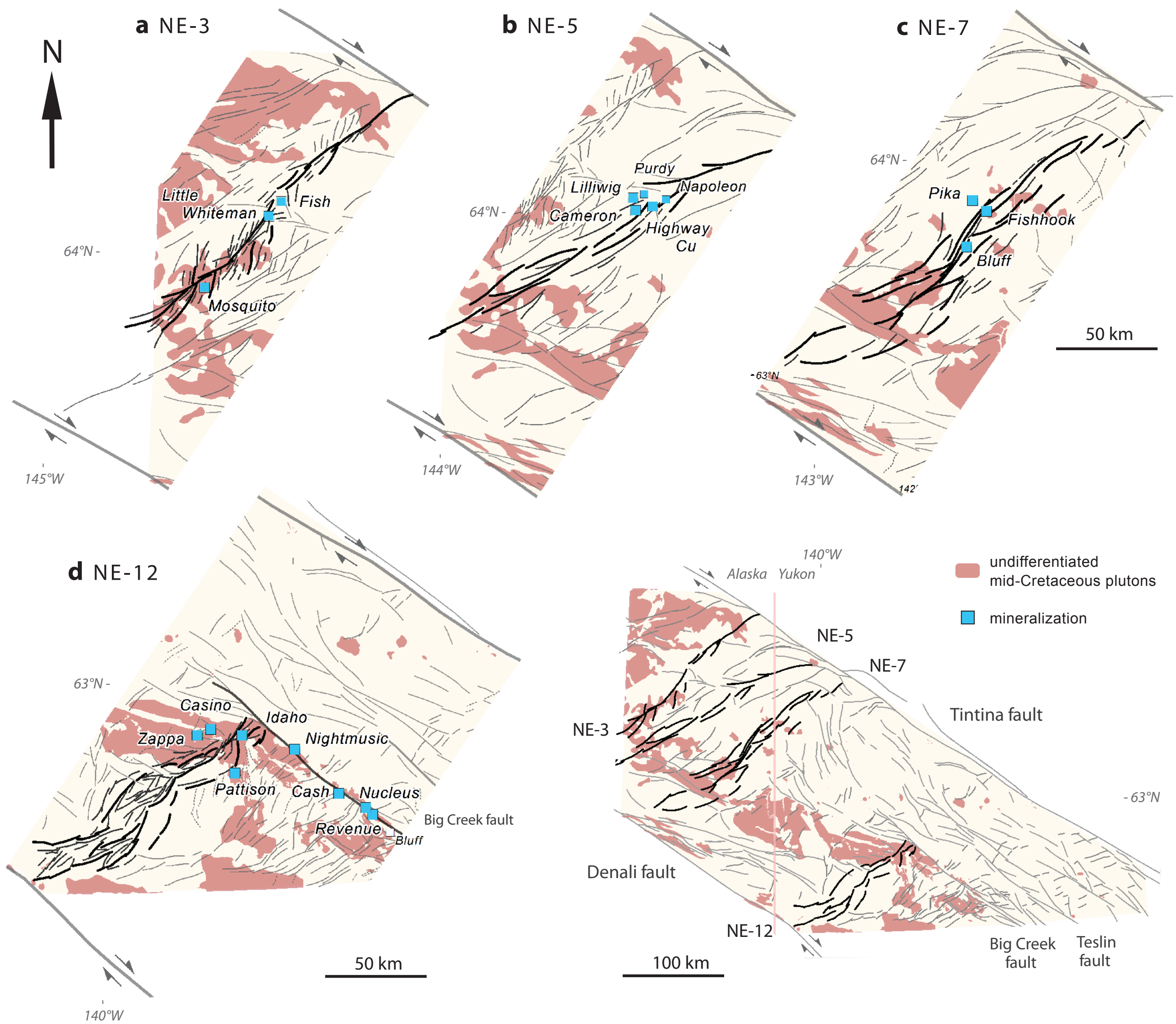

Figure 4. *Key examples of northeast-striking magnetic discontinuities, distribution of mid-Cretaceous plutons, and mainly Cretaceous magmatic-hydrothermal mineralization. The Alaska area shows continuous and linear northeast-trending "mag-breaks" (a, b, c), whereas the Yukon area is characterized by increased along-strike segmentation (d). Location map in bottom right corner. Mid-Cretaceous plutonic rocks modified from Gordey et al., 2005; Ryan et al., 2010; Beikman et al., 1980; and Gordey and Makepeace, 1999.*

YUKON AREA

Towards the center and south-eastern portion of the RTP magnetic grid and east of the Alaska-Yukon border, northeast-southwest oriented, magnetite-destructive lineaments display increasingly curvilinear geometry and increased along-strike segmentation (Figs. 3 and 4). These systems of linear magnetic discontinuities are frequently composed of a series of individual segments of 10 to 50 km in length that are interpreted to link and relay along strike. North of the Dawson Range, all five major structural corridors (NE-9 to NE-13 in Fig. 3) appear truncated by at least two major northwest-southeast oriented regional magnetic discontinuities. These correspond to the Big Creek and Teslin faults, both major, dextral, strike-slip structures of mid to Late Cretaceous age (Fig. 4; Colpron *et al.*, 2007; Gabrielse *et al.*, 2006).

The northeast-oriented Dip Creek fault (Johnston, 1999) is the most prominent orogen-perpendicular magnetic truncation of the Yukon area (Fig. 4d). We interpret this fault as extending for ~130 km from near the Denali fault to the northern flank of the Dawson Range, where it terminates immediately south of the Big Creek fault. The Dip Creek fault is interpreted as a highly segmented structural corridor composed of arcuate border faults and internal faults. This fault zone is up to ~16 km wide, with its narrower northeastern section generating a major offset across the Dawson Range batholith (Fig. 4d). In addition to the Dip Creek fault system, at least five other prominent examples of segmented northeast-southwest discontinuities are interpreted south of the Big Creek fault across the Dawson Range (Fig. 3).

IMPLICATIONS FOR MINERALIZATION

At the scale of the current interpretation, a number of established mid to Late Cretaceous porphyry and hydrothermal mineral occurrences and deposits cluster along the arc-perpendicular structures defined in this study (Figs. 4 and 5). These magnetic lineaments are interpreted to define zones of increased structural damage and enhanced permeability, which may consequently focus mid to Late Cretaceous magmatism, hydrothermal activity, and mineralization. While the northeast-southwest structures may represent a first order structural control across the Alaskan quadrant, a weaker, secondary role is interpreted for the Yukon segment of the Dawson Range. The most obvious correlations between northeast-trending structures and Late Cretaceous porphyry and polymetallic vein occurrences occur along the NE-3 (Ketchumstuk fault) and NE-7 structural corridors of the Fortymile and Sixtymile areas (Figs. 4a,c). A more complex scenario occurs along the Dawson Range, with examples of second order structural controls from the NE-12 zone of the Dip Creek fault (Fig. 4d).

ALASKAN AREA

Along the Ketchumstuk fault of the Fortymile District (Szumigala *et al.*, 2003), or in close proximity to it, a series of known mid to Late Cretaceous magmatic-related mineral occurrences and deposits occur (Fig. 4a). Known Cretaceous deposits along the western segment of NE-3 include the 70.5 Ma Fish massive sulphide prospect (Ag, Cu, Pb, Zn) (Dusel-Bacon *et al.*, 2007; Full Metal Minerals, 2012). The Little Whiteman carbonate replacement prospect (Zn, Pb, Ag) and the Mosquito porphyry Cu-Mo prospect may also be of similar age (Cox and Singer, 1986). Further examples of Cretaceous magmatic-related mineralization and northeast trending faults occur at the NE-7 of the Sixtymile River area in the vicinity of the Yukon/Alaska border (Fig. 4c). These include the Bluff/Taurus and Pika Canyon Cu-Mo-Au porphyry deposits (Cox and Singer, 1986), as well as the Fishhook Ag-Au (barite, Cu, Mo, Pb, Sb) prospect (http://www.mindat.org/loc-197486.html). A major cluster of age-unconstrained, magmatic-related lode gold mineralization and associated placer gold deposits occur where NE-5 intersects with a major northwest-trending magnetic discontinuity (Fig. 4b). Here, intrusion-related mineralization occurs in the Cameron (Chicken West; Opal), Highway Copper (Bruce), and Lilliwig Creek prospects, as well as a number of unnamed occurrences (Alaska ARDF, 2012). The Napoleon shear-hosted gold prospect (Werdon *et al.*, 2001) and Purdy epithermal gold veins (Cox and Singer (eds.), 1986) have been assigned an Early Jurassic mineralization age (*ibid*).

YUKON AREA

In central Yukon, the northwest-trending Big Creek fault controls the distribution of mid to Late Cretaceous magmatism and generates a highly linear magnetic discontinuity and morphologic trench which extends for ~120 km along the northeastern flank of the Dawson Range (Figs. 4 and 5). This dextral fault system exerts a first-order structural role in the emplacement of Late Cretaceous deposits and occurrences (Bennett *et al.*, 2010). Notable examples include the Cash (Cu, Mo) porphyry (Selby and Creaser, 2001), the Nightmusic zone of the Sonora Gulch porphyry prospect (Northern Tiger, 2012), and the Nucleus and Revenue Au porphyries (Northern Freegold, 2012a,b; Fig. 4d). Although northeast-southwest structures appear to play a secondary role in the area, their intersection with the Big Creek fault may generate zones of enhanced permeability and mineralization. The Dip Creek fault (NE-12), the most significant northeast-trending fault in the area, dislocates the mid-Cretaceous Dawson Range batholith and shows a regional-scale correlation with a series of Late Cretaceous porphyry-related systems (Figs. 4d and 5). Examples include: the mid-Cretaceous Idaho Au-Ag vein zone, Pattison Cu-Mo porphyry prospect, the Zappa Cu porphyry-style anomaly, and most notably, the Late Cretaceous Casino Cu-Mo-Au porphyry deposit (Fig. 4d; Selby and Creaser, 2001).

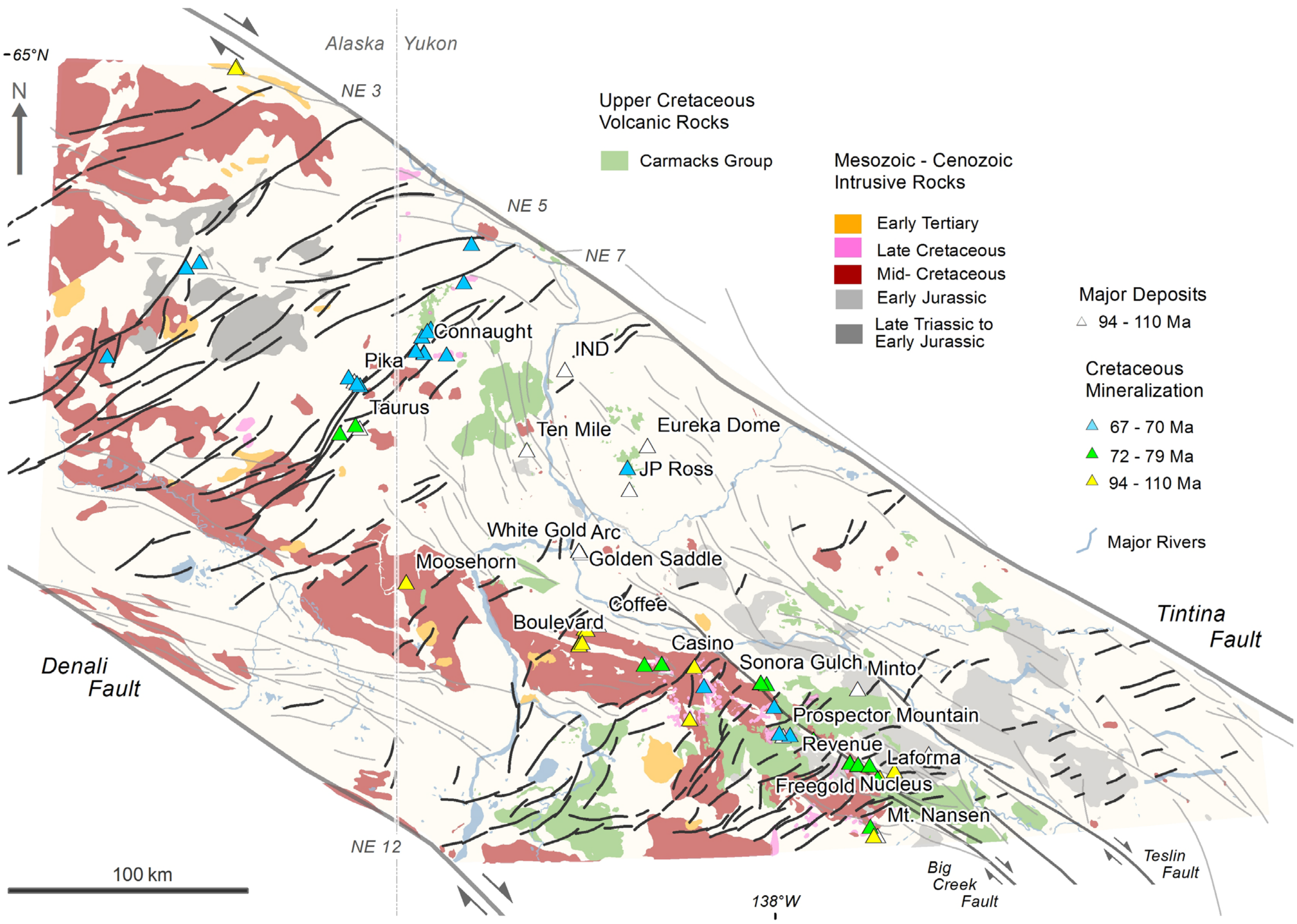

Figure 5. *Simplified geological map showing the along-strike northeast-trending segmentation of Mesozoic geologic units and the spatial distribution of major mineral deposits and mid to Late Cretaceous magmatic-hydrothermal mineralization (modified from Gordey et al., 2005; Ryan et al., 2010; Beikman et al., 1980; and Gordey and Makepeace, 1999). Magnetic discontinuities and geological offsets are most commonly observed across the mid-Cretaceous igneous arc and Upper Cretaceous Carmacks Group volcanics.*

DISCUSSION

We infer that the series of magnetite-destructive linear discontinuities interpreted from the reduced-to-pole grid (Buckingham and Core, 2012), correlate with steeply-dipping brittle fault systems of post-Jurassic age. Several of these discontinuities have been mapped as faults in regional geologic maps, although a much larger number of faults are inferred from the current study. Evidence of along-strike fault-block segmentation by northeast-trending magnetite-destructive discontinuities include: (1) abrupt variations in the orientation of geological contacts and map-view exposure of intrusive units; (2) map-view linear offsets of major geological units (e.g., Dawson Range batholith); (3) distribution of sedimentary basins (e.g., Paleogene volcano-sedimentary sediments) and volcanic units (e.g., Carmacks Group volcanics); and (4) the presence and offsets of geomorphologic trenches and ridges, as well as river systems (Fig. 5). In accordance to their linear geometry, these northeast-trending structural systems are interpreted as steep, brittle extensional, oblique-extensional or strike-slip fault systems. Their regional dimensions, regular spacing, and similar magnetic character and geometries suggest that they arise from a common tectonic process.

Structural controls on hydrothermal and subvolcanic ore systems largely derive from the role that deformation processes and fluid pressures play on generating and maintaining permeability within active faults, shear zones, and associated fracture networks, at various crustal levels (Cox, 1999; Micklethwaite and Cox, 2004; Berger, 2007; Sibson, 1987). We infer that steeply dipping, northeast-trending, brittle structures have focused pervasive fracturing with the capability to generate a substantial increase in rock permeability and pressure gradients. Secondary permeability may be further enhanced at structural intersections with regional fault systems which controlled mid-Cretaceous magmatism (*e.g.*, Big Creek fault). World-class examples of magmatic hydrothermal Cu-Au deposits, located at zones of intersection between oblique structures and younger structurally-controlled magmatic arcs, have been proposed for the middle Eocene to early Oligocene metallogenic belt of northern Chile (Richards *et al.*, 2001; Richards, 2003; Sillitoe and Perello, 2005; Sillitoe, 2010). Within this belt, gigantic porphyry deposits (*e.g.*, La Escondida, El Salvador, Chiquicamata) and epithermal systems (*e.g.*, Pascua Lama, La Coipa) cluster at the junction of northwest-trending basement segments with north-south oriented magmatic arcs and structural systems (*e.g.*, West Fissure). In a similar manner to the northern Chilean Andes, the identification of structural systems, crosscutting at high angles to the mid-Cretaceous Dawson Range arc and regional fault systems, may provide relevant criteria for targeting porphyry and epithermal ore systems in the Northern Cordillera.

CONCLUSION

Northeast-oriented structures, as interpreted from a series of linear magnetic discontinuities, are orientated semi-perpendicularly to the regional northwest-trending magnetic grain, mid-Cretaceous magmatic arc, and overall Mesozoic to Cenozoic structural architecture. These magnetite-destructive corridors are interpreted as steeply dipping brittle fault zones and fracture arrays of extensional, oblique-extensional, and strike-slip kinematics, responsible for localized structural damage and along-strike block segmentation. Within these structural systems, substantial increments in rock permeability, fluid flow, and pressure gradients may favour the generation of mid to Late Cretaceous hydrothermal veins and subvolcanic stocks.

At the scale of observation in the current study, the spatial correlation between northeast-oriented steep dipping structural systems and known mid to Late Cretaceous magmatic-hydrothermal mineral deposits and occurrences suggests a first-order structural control in eastern Alaska. Arc-parallel structures like the Big Creek fault exert the first-order structural control on magmatic-hydrothermal systems in the Dawson Range, but northeast structures such as the Dip Creek fault system may play a second-order role. The relationship of northeast-oriented structures to exposures of Carmacks Group volcanic rocks and mineral prospects of known Late Cretaceous age, suggests that these structures were mainly active in Late Cretaceous time.

ACKNOWLEDGEMENTS

Funding for this research has been provided by grants from Natural Resources Canada (NRCan) and from the Natural Sciences and Engineering Research Council of Canada (NSERC). Additional support has been provided by the Yukon Gold Project, a collaborative research venture between the Mineral Deposit Research Unit (The University of British Columbia) and a consortium of industry participants. The authors are also grateful to Steve Israel for helpful comments on this manuscript.

REFERENCES

Alaska ARDF, 2012. Resource Data File - Alaska (ARDF). Alaska ARDF on the web, https://explore.data.gov/Geography-and-Environment/Resource-Data-File-Alaska-ARDF-/f9ps-ajhr, retrieved December, 20, 2012.

Baker, T. and Lang, J.R., 2001. Fluid inclusion characteristics of intrusion-related gold mineralization, Tombstone-Tungsten magmatic belt, Yukon Territory, Canada. Mineralium Deposita, vol. 36, p. 563-582.

Beikman, H.M., 1980. Geologic map of Alaska. U.S. Geological Survey, 1:2 500 000.

Bennett, V., Colpron, M., and Burke, M., 2010. Current thinking on Dawson Range Tectonics and Metallogeny. Yukon Geological Survey, Miscellaneous Report MR-2.

Berger, B.R., 2007. The 3D fault and vein architecture of strike-slip releasing- and restraining bends: evidence from volcanic-centre-related mineral deposits. Geological Society, London, Special Publications, vol. 290, p. 447-471.

Buckingham, A. and Core, D., 2012. Enhancement Filtering and Structure Detection Magnetic and Gravity Data, MDRU Project Area Yukon Alaska. Fathom Geophysics, internal report.

Clark, D., 1999. Magnetic petrology of igneous intrusions: implications for exploration and magnetic interpretation. Exploration Geophysics, vol. 30, p. 5–26.

Clark, D., Geuna, S., and Schmidt, P., 2004. Predictive magnetic exploration models for porphyry, epithermal, and iron oxide copper-gold deposits: implications for exploration. AMIRA International Ltd., P700 Final Report.

Colpron, M. and Nelson, J.L., 2011. A Digital Atlas of Terranes for the Northern Cordillera. British Columbia Geological Survey, GeoFile 2011-11.

Colpron, M., Nelson, J.L., and Murphy, D.C., 2007. Northern Cordilleran terranes and their interactions through time. GSA Today, vol. 17, p. 4-10.

Cooke, D.R., McPhail, D.C., and Bloom, M.S., 1996. Epithermal gold mineralization, Acupan, Baguio District, Philippines; geology, mineralization, alteration, and the thermochemical environment of ore deposition. Economic Geology, vol. 91, p. 243-272.

Cordey, F., Mortimer, N., DeWever, P., and Monger, J.W.H., 1987. Significance of Jurassic radiolarians from the Cache Creek terrane, British Columbia. Geology, vol. 15, p. 1151-1154.

Cox, S.F., 1999. Deformational controls on the dynamics of fluid flow in mesothermal gold systems. Geological Society, London, Special Publications, vol. 155, p. 123-140.

Cox, S.F. and Ruming, K., 2004. The St Ives mesothermal gold system, Western Australia—a case of golden aftershocks? Journal of Structural Geology, vol. 26, p. 1109-1125.

Cox D.P. and Singer D.A. (eds.), 1986. Mineral Deposit Models. US Geological Survey, Bulletin 1693, 379 p.

Crawford, B.L., Betts, P.G., and Aillères, L., 2010. An aeromagnetic approach to revealing buried basement structures and their role in the Proterozoic evolution of the Wernecke Inlier, Yukon Territory, Canada. Tectonophysics, vol. 490, p. 28-46.

Domzalski, W., 1966. Importance of Aeromagnetics in Evaluation of Structural Control of Mineralization. Geophysical Prospecting, vol. 14, p. 273-291.

Dusel-Bacon, C., Lanphere, M.A., Sharp, W.D., Layer, P.W., and Hansen, V.L., 2002. Mesozoic thermal history and timing of structural events for the Yukon-Tanana Upland, east-central Alaska: 40Ar/39Ar data from metamorphic and plutonic rocks. Canadian Journal of Earth Sciences, vol. 39, p. 1013-1051.

Dusel-Bacon, C., Slack, J.F., Aleinikoff, J.N., and Mortensen, J.K., 2007. Mesozoic magmatism and base-metal mineralization in the Fortymile mining district, eastern Alaska: initial results of petrographic, geochemical, and isotopic studies in the Mount Veta area. US Geological Survey, Professional Paper 1760-A, 50 p.

Full Metal Minerals, 2012. Full Metal Discovers a Second Massive Sulphide System at 40 Mile. Full Metal Minerals on the Web, http://www.fullmetalminerals.com/380/, retrieved December 20, 2012.

Gabrielse, H., 1985. Major dextral transcurrent displacements along the Northern Rocky Mountain Trench and related lineaments in north-central British Columbia. Geological Society of America, Bulletin 96, p. 1-14.

Gabrielse, H., Murphy, D.C., and Mortensen, J.K., 2006. Cretaceous and Cenozoic dextral orogen-parallel displacements, magmatism, and paleogeography, north-central Canadian Cordillera. *In:* Paleogeography of the North American Cordillera: Evidence For and Against Large-Scale Displacements, J.W. Haggart, R.J. Enkin, and J.W.H. Monger (eds.), Geological Association of Canada, Special Paper 46, p. 255-276.

Garrity, C.P. and Soller, D.R., 2009. Database of the Geologic Map of North America; adapted from the map by J.C. Reed, Jr. and others (2005), 1:5 000 000. U.S. Geological Survey Data Series 424, http://pubs.usgs.gov/ds/424/.

Gordey, S.P. and Makepeace, A.J. (comps.), 1999. Yukon Digital Geology. Indian & Northern Affairs Canada/ Department of Indian & Northern Development: Exploration & Geological Services Division, Open File 1999-1(D).

Gordey, S.P. and Ryan, J.J., 2005. Geology, Stewart River Area (115 N, 115 O, and part of 115 J), Yukon Territory. Geological Survey of Canada, Open File 4970, 1:250 000.

Grant, F.S., 1985. Aeromagnetics, geology and ore environments, I. Magnetite in igneous, sedimentary and metamorphic rocks: an overview. Geoexploration, vol. 23, p. 303-333.

Gunn, P. and Dentith, M., 1997. Magnetic responses associated with mineral deposits. AGSO Journal of Australian Geology and Geophysics vol. 17, p. 145–158.

Hart, C.J., Goldfarb, R.J., Lewis, L.L., and Mair, J.L., 2004. The Northern Cordilleran Mid-Cretaceous Plutonic Province: Ilmenite/Magnetite-series Granitoids and Intrusion-related Mineralization. Resource Geology, vol. 54, p. 253-280.

Hayward, N., Miles, W., and Oneschuk, D., 2011. Geophysical Series, regional geophysical compilation project, Yukon Plateau, Yukon, parts of NTS 105, 106, 115 and 116. Geological Survey of Canada, Open File 6959.

Hedenquist, J.W., Izawa, E., Arribas, A., and White, N.C., 1996. Epithermal gold deposits: Styles, characteristics, and exploration. Resource Geology Special Publication Number 1. Society of Resource Geology, Japan, 16 p.

Henley, R.W. and Adams, D.P.M., 1992. Strike-slip fault reactivation as a control on epithermal vein-style gold mineralization. Geology, vol. 20, p. 443-446.

Izawa, E., Urashima, Y., Ibaraki, K., Suzuki, R., Yokoyama, T., Kawasaki, K., Koga, A. and Taguchi, S., 1990. The Hishikari gold deposit: high-grade epithermal veins in Quaternary volcanics of southern Kyushu, Japan. Journal of Geochemical Exploration, vol. 36, p. 1-56.

Johnston, S.T., 1999. Large-scale coast-parallel displacements in the Cordillera: a granitic resolution to a paleomagnetic dilemma. Journal of structural geology, vol. 21, p. 1103-1108.

Logan, J.M., Schiarizza, P., Struik, L.C., Barnett, C., Nelson, J.L., Kowalczyk, P., Ferri, F., Mihalynuk, M.G., Thomas, M.D., Gammon, P., Lett, R., Jackaman, W., and Ferbey, T., 2010. Geoscience Map 2010-1: Bedrock Geology of the QUEST map area, central British Columbia. Geological Survey of Canada, Open File 6476.

Lund, K., 2008. Geometry of the Neoproterozoic and Paleozoic rift margin of western Laurentia: Implications for mineral deposit settings. Geosphere, vol. 4, p. 429.

Mair, J.L., Hart, C.J., and Stephens, J.R., 2006. Deformation history of the northwestern Selwyn Basin, Yukon, Canada: Implications for orogen evolution and mid-Cretaceous magmatism. Geological Society of America, Bulletin 118, p. 304-323.

McMechan, M.E., 2012. Deep transverse basement structural control of mineral systems in the southeastern Canadian Cordillera. Geological Survey of Canada, Contribution 20110294. Canadian Journal of Earth Sciences, vol. 49, p. 693-708.

Micklethwaite, S. and Cox, S.F., 2004. Fault-segment rupture, aftershock-zone fluid flow, and mineralization. Geology, vol. 32, p. 813-816.

Micklethwaite, S., Sheldon, H.A., and Baker, T., 2010. Active fault and shear processes and their implications for mineral deposit formation and discovery. Journal of Structural Geology, vol. 32, p. 151-165.

Mihalynuk, M.G., Nelson, J., and Diakow, L.J., 1994. Cache Creek terrane entrapment: Oroclinal paradox within the Canadian Cordillera. Tectonics, vol. 13, p. 575-595.

Mihalynuk, M.G., Smith, M.T., Gabites, J.E., Runkle, D., and Lefebure, D., 1992. Age of emplacement and basement character of the Cache Creek terrane as constrained by new isotopic and geochemical data. Canadian Journal of Earth Sciences, vol. 29, p. 2463-2477.

Mortensen, J.K., 1992. Pre-Mid-Mesozoic tectonic evolution of the Yukon-Tanana terrane, Yukon and Alaska. Tectonics, vol. 11, p. 836-853.

Mortensen, J.K., Hart, C.J.R., Murphy, D.C., and Heffernan, S., 2000. Temporal evolution of Early and mid-Cretaceous magmatism in the Tintina Gold Belt. *In:* The Tintina Gold Belt: Concepts, Exploration and Discoveries, T.L. Tucker and M.T. Smith (eds.), Vancouver, British Columbia and Yukon Chamber of Mines, Cordilleran Roundup, Special Volume 2, p. 49-57.

Nabighian, M.N., Grauch, V.J.S., Hansen, R.O., LaFehr, T.R., Li, Y., Peirce, J.W., Phillips, J.D., and Ruder, M.E., 2005. 75th Anniversary: The historical development of the magnetic method in exploration. Geophysics, vol. 70, p. 33ND-61ND.

Nelson, J.L., Colpron, M., Piercey, S.J., Dusel-Bacon, C., Murphy, D.C., and Roots, C.F., 2006. Paleozoic tectonic and metallogenic evolution of the pericratonic terranes in Yukon, northern British Columbia and eastern Alaska. *In:* Paleozoic Evolution and Metallogeny of Pericratonic Terranes at the Ancient Pacific Margin of North America, Canadian and Alaskan Cordillera, M. Colpron, and J.L. Nelson, (eds.), Geological Association of Canada, Special Paper 45, p. 323-360.

Northern Freegold, 2012a. Northern Freegold Extends the Nucleus Gold Deposit. Northern Freegold Resources on the web, http://www.northernfreegold.com/s/NewsReleases.asp?ReportID=551882, retrieved December 20, 2012.

Northern Freegold, 2012b. Northern Freegold Files Revenue Deposit NI 43-101 Technical Report at Freegold Mountain. Northern Freegold Resources on the web, http://www.northernfreegold.com/s/NewsReleases.asp?ReportID=511840, retrieved December 20, 2012.

Northern Tiger, 2012. Sonora Gulch Project. Northern Tiger Resources on the web, http://www.northern-tiger.com/s/Sonora.asp, retrieved December 20, 2012.

Pilkington, M. and Saltus, R.W., 2009. The Mackenzie River magnetic anomaly, Yukon and Northwest Territories, Canada—Evidence for Early Proterozoic magmatic arc crust at the edge of the North American craton. Tectonophysics, vol. 478, p. 78-86.

Pilkington, M., Snyder, D.B., and Hemant, K., 2006. Weakly magnetic crust in the Canadian Cordillera. Earth and Planetary Science Letters, vol. 248, p. 476-485.

Purucker, M.E. and Clark, D.A., 2011. Mapping and Interpretation of the Lithospheric Magnetic Field. Geomagnetic Observations and Models, vol. 5, p. 311-337.

Richards, J.P., 2003. Tectono-Magmatic Precursors for Porphyry Cu-(Mo-Au) Deposit Formation. Economic Geology, vol. 98, p. 1515-1533.

Richards, J.P., Boyce, A.J., and Pringle, M.S., 2001, Geological evolution of the Escondida area, northern Chile: A model for spatial and temporal localization of porphyry Cu mineralization. Economic Geology, vol. 96, p. 271–305.

Ryan, J.J., Colpron, M., and Hayward, N., 2010. Geology, southwestern Mcquesten and parts of northern Carmacks, Yukon. Geological Survey of Canada, Canadian Geoscience Map 7 (preliminary version), 1:125 000.

Saltus, R.W., 2007. Matching magnetic trends and patterns across the Tintina fault, Alaska and Canada - Evidence for offset of about 490 kilometers *In:* Recent U.S. Geological Survey Studies in the Tintina Gold Province, Alaska, United States, and Yukon, Canada. Results of a 5-Year Project, L.P. Gough, and W.C. Day, (eds.), U.S. Geological Survey, Scientific Investigations Report 2007-5289-C, 7 p.

Sandrin, A., Berggren, R., and Elming, S., 2007. Geophysical targeting of Fe-oxide Cu-(Au) deposits west of Kiruna, Sweden. Journal of Applied Geophysics, vol. 61, p. 92–101.

Selby, D. and Creaser, R.A., 2001. Late and mid-Cretaceous mineralization in the northern Canadian Cordillera: Constraints from Re-Os molybdenite dates. Economic Geology, vol. 96, p. 1461-1467.

Sibson, R.H., 1987. Earthquake rupturing as a mineralizing agent in hydrothermal systems. Geology, vol. 15, p. 701-704.

Sillitoe, R.H., 1997. Characteristics and controls of the largest porphyry copper-gold and epithermal gold deposits in the circum-Pacific region. Australian Journal of Earth Sciences, vol. 44, p. 373-388.

Sillitoe, R.H. and Perelló, J., 2005. Andean copper province: Tectonomagmatic settings, deposit types, metallogeny, exploration, and discovery. Economic Geology, 100th Anniversary Volume, p. 845–890.

Sillitoe, R.H., 2010. Porphyry copper systems. Economic Geology, vol. 105, p. 3-41.

Szumigala, D.J., Hughes, R.A., and Harris, R.H., 2003. Alaska Mineral Industry 2003. Division of Geological and Geophysical Survey, Fairbanks, Alaska, Special Report 58.

Van Leeuwen, T.M., Leach, T., Hawke, A.A., and Hawke, M.M., 1990. The Kelian disseminated gold deposit, east Kalimantan, Indonesia. Journal of Geochemical Exploration, vol. 35, p. 1-61.

Vikre, P.G., 1989. Fluid-mineral relations in the Comstock Lode. Economic Geology, vol. 84, p. 1574-1613.

Werdon, M.B., Newberry, R.J., Szumigala, D.J., and Burns, L.E., 2001. Reconnaissance bedrock geology of the Pogo area, Big Delta B-2 and B-3 Quadrangles, Alaska. Alaska Division of Geological and Geophysical Surveys, Preliminary Interpretive Report 2001-5, 1:63 360.

Willis, G.F. and Tosdal, R.M., 1992. Formation of gold veins and breccias during dextral strike-slip faulting in the Mesquite mining district, southeastern California. Economic Geology, vol. 87, p. 2002-2022.